Percutaneous Translumbar Spinal Cord Compression Injury in a Dog Model That Uses Angioplasty Balloons: MR Imaging and Histopathologic Findings

Phillip D. Purdy, Robert T. Duong, Charles L. White III, Donna L. Baer, R. Ross Reichard, G. Lee Pride, Jr., Christina Adams, Susan Miller, Christa L. Hladik and Zerrin Yetkin

AJNR Am J Neuroradiol 2003, 24 (2) 177-184
http://www.ajnr.org/content/24/2/177

AJNR Am J Neuroradiol 24:177–184, February 2003

Percutaneous Translumbar Spinal Cord Compression Injury in a Dog Model That Uses Angioplasty Balloons: MR Imaging and Histopathologic Findings

Phillip D. Purdy, Robert T. Duong, Charles L. White, III, Donna L. Baer, R. Ross Reichard, G. Lee Pride, Jr., Christina Adams, Susan Miller, Christa L. Hladik, and Zerrin Yetkin

BACKGROUND AND PURPOSE: **Previous animal models for spinal cord injury required laminectomy and exposure of the spinal cord to create direct trauma, compromising imaging by both surgical artifact and the nature of the production of the injury. Our purpose was to study a model that uses percutaneous intraspinal navigation with an angioplasty balloon, providing a controlled degree of spinal cord compression and allowing improved MR imaging of spinal cord injury.**

METHODS: **Nine mongrel dogs were studied. MR images were obtained of six dogs after technique development in three dogs. Angioplasty balloons measuring 7 or 4 mm in diameter and 2 cm in length were placed in the midthoracic subarachnoid space. Imaging was performed by using a 1.5-T MR imaging unit before and after balloon inflation. The balloon was inflated within 5 seconds and deflated after 30 minutes. T1- and T2-weighted and contrast-enhanced images were acquired. Spinal cords were submitted for pathologic examination.**

RESULTS: **All four animals with 7-mm balloons experienced hemorrhage, and three had axonal injury revealed by histopathologic examination. One of two animals with 4-mm balloons experienced no injury, and one had axonal injury without hemorrhage. Regional parenchymal enhancement was seen in two of the animals with 7-mm balloons.**

CONCLUSION: **This percutaneous spinal cord injury model results in a graduating degree of injury. It differs from previous techniques by avoiding surgical exposure and the associated artifacts, yet it offers histopathologic findings similar to those of human spinal cord injury. The canine spinal cord is amenable to MR imaging with clinical imaging units. Further evaluations with various durations of compression and various balloon sizes are warranted.**

Models for spinal cord injury research have historically most frequently involved surgical exposure of the spinal cord. The impact model, and variants thereof, which was first described by Allen in 1911 (1), involved the dropping of a predetermined weight from a predetermined height onto an exposed spinal cord. It produced a known trauma and carried the advantage of the production of a "shock" injury to the spinal cord (2–9). Fukuoka et al (10) used a sublaminar surgical implantation called *laminaria* in rats. Laminaria is a material that swells when implanted. Other mechanisms have included weights (11–13) or aneurysm clips (14) placed on the cord from an extradural exposure, subpial injection of an excitotoxic compound (15), and a pneumatic device (16, 17) or compression apparatus (18) to apply compression over a laminectomy site in rats (16, 17). In all these models, however, the open exposure of the spinal cord was nonphysiological and immediate imaging was compromised both by surgical artifact and by the nature of the production of the injury.

Rodents and other small animals are economically and readily available. However, for imaging studies

Received January 3, 2002; accepted after revision September 5.

This work was funded in part by The University of Texas Southwestern Mobility Foundation Center, University of Texas Southwestern Medical Center at Dallas, Dallas, TX.

From the Department of Radiology (Division of Neuroradiology) (P.D.P., R.T.D., G.L.P., Z.Y.), the Department of Neurological Surgery (P.D.P.), the Department of Pathology (Division of Neuropathology) (C.L.W., R.R.R.), the Animal Resources Center (D.L.B.), the Mobility Foundation Center (P.D.P., C.A., S.M., Z.Y.), and the Department of Pathology (Immunohistochemistry Laboratories) (C.L.H.), The University of Texas, Southwestern Medical Center at Dallas, Dallas, TX.

Address reprint requests to Phillip D. Purdy, MD, University of Texas Southwestern Medical Center, 5323 Harry Hines Boulevard, Dallas, TX 75390.

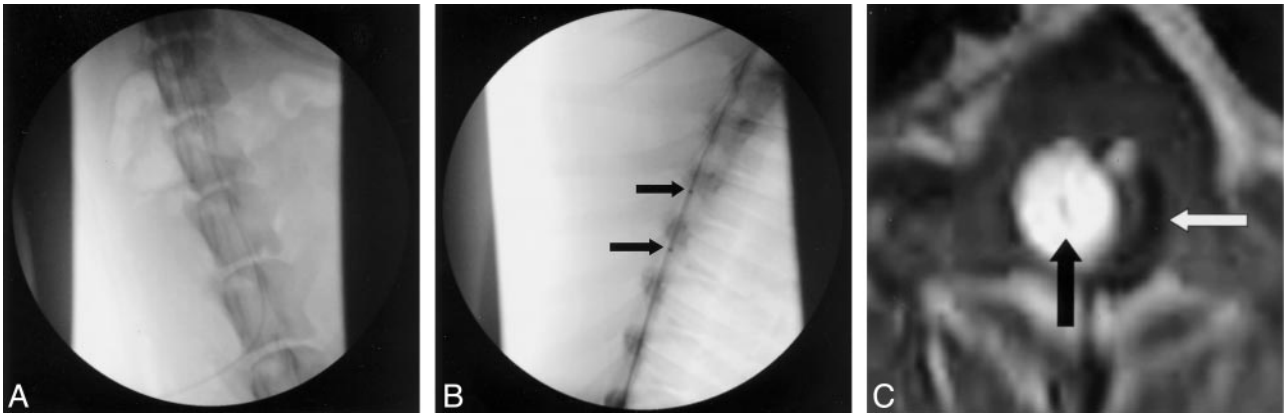

FIG 1. Images from a pilot study. After induction of general endotracheal anesthesia, the lumbar subarachnoid space was entered with a needle. A guidewire was introduced via the needle and directed cephalad; then, the needle was withdrawn, and the guidewire was used for coaxial advancement of the angioplasty balloon, mimicking the method used in vascular access for angiography.

A, Guidewire introduced via neural foramen (lateral approach) and ascending in spinal canal.

B, Angioplasty balloon introduced over guidewire. Proximal and distal markers on balloon are shown by *arrows*.

C, Example of an MR image of a 7-mm balloon (*black arrow*) inflated against the compressed spinal cord in animal 2 (*white arrow*).

and/or therapeutic interventions that translate readily to the clinical setting, larger animals are more analogous to humans. It is not feasible to achieve satisfactory resolution when imaging small animal spinal cords by using instruments intended for humans (meter bore 1.5-T systems). We sought to develop a model that did not require open exposure of the spinal cord and that would be able to deliver a variable yet controlled degree of spinal cord compression in a species large enough for a standard 1.5-T MR imaging unit. We herein present a canine model that uses a percutaneously introduced angioplasty balloon in the spinal subarachnoid space to create injury.

Methods

A total of nine mongrel dogs that were unselected regarding age and sex and that weighed between 18 and 36 kg represented the study cohort. Of these, three served as a source of pilot data to develop the technique and were studied without MR imaging. Six were studied with MR imaging after the placement of a deflated balloon next to the midthoracic spinal cord. They were transferred to the MR imaging unit before balloon inflation. Those six served as sources for the data reported in this study.

The concept of this technique was investigated first in an animal from another protocol after it was killed. With that animal, it was discovered that direct lateral puncture represented a viable approach to the spinal subarachnoid space (via a lateral foramen in the lumbar spine). Thus, it was possible, under fluoroscopic guidance, to perform a lumbar puncture via a due lateral approach that traversed the paraspinous muscle.

Subsequently, after obtaining approval from the Institutional Animal Care and Research Advisory Committee, pilot studies were performed in three study animals in which, after induction of general endotracheal anesthesia, the lumbar subarachnoid space was entered with a needle and a guidewire was introduced by using a technique that mimicked the method used in vascular access for angiography (Fig 1A). It was possible, under fluoroscopic guidance, to control and direct the guidewire either anterior or posterior to the spinal cord. Once the guidewire was placed, the tract was dilated by using a 5F dilator that is routinely used for angiography. The dilator was introduced into the subarachnoid space, fully dilating the dural entry point, and was then removed, leaving the wire in place. A 5F dual-lumen catheter with an angioplasty balloon that was 2 cm long on its distal tip was then introduced into the subarachnoid space. The balloon catheter/guidewire was advanced, again under fluoroscopic guidance, until it was in the midthoracic spine (Fig 1B). In that location, the balloon was inflated by using half-strength contrast material. It was left inflated for 30 minutes and was then deflated. The animal was supported under continued anesthesia for a total observation period of 4 hours, after which it was killed. An autopsy to remove the spinal cord was undertaken.

After the pilot studies, an additional six animals were studied in which the procedure quoted above was followed, except that after balloon placement and before inflation, the animal was transported to our MR imaging research center and placed on a 1.5-T MR imaging unit. All balloons were placed in the thoracic canal in the T6–T7 region. After obtaining baseline images to localize the balloon, the balloon was inflated within 5 seconds with a dilute contrast solution and was left inflated for 30 minutes (Fig 1C). After 30 minutes, the balloon was deflated and the animal was left in position in the imaging unit for an additional period of 1.5 to 2.75 hours (total MR imaging time, 4 hours) and continuous imaging was performed. Near the end of the imaging time, contrast material was IV administered and contrast-enhanced images were obtained.

Before placement in the magnet, animals were monitored with EKG and a pulse oximeter. After placement in the magnet, however, we were able to monitor only the heart rate. Animals were mechanically ventilated throughout the experiment with a mixture of oxygen and Fluothane. Neuromuscular blockade was maintained pharmacologically.

For imaging, the animal was placed in the left lateral decubitus position. The surface coil was located on the marked region of the spinal column overlying the balloon catheter. Images of the spinal region were acquired in the coronal, axial, and sagittal planes encompassing the region 1 cm above and below the balloon. T1-weighted images (600/13 [TR/TE]; number of sections acquired, 28; section thickness, 4 mm with section gap of 0.4 mm to increase coverage) were obtained during inflation of the balloon. T1- and T2-weighted images (2227/85; number of sections acquired, eight; section thickness, 4 mm with section gap of 0.4 mm to increase coverage) were obtained after deflation of the balloon. After the IV administration of 0.2 mmol/kg contrast material, T1-weighted images were acquired to evaluate the contrast enhancement in the spinal cord.

For all animals, the degree of balloon expansion was evaluated based on T1-weighted images. Quantitative assessment of

TABLE 1: Summary of MR imaging and neuropathological findings

Animal #	Compression (min)	Balloon Size (mm)	Hemorrhage	APP	Enhancement	T1	T2	SCO %
1	30	4	Negative	Negative	Negative	Negative	Negative	29
2	30	4	Negative	Positive	Negative	Positive	Negative	31
3	30	7	Positive	Positive	Positive	Negative	Negative	79
4	30	7	Positive	Positive	Negative	Negative	Negative	62
5	30	7	Positive	Positive	Positive	Positive	Negative	67
6	30	7	Positive	Negative	Negative	Positive	Negative	69

Note.—APP indicates amyloid precursor protein.

balloon expansion was accomplished by using an off-line software program. The extent of spinal canal occlusion was determined by the percentage of the ratio of the balloon area to the spinal canal. All images were assessed for indication of injury to the spinal cord, including increased signal intensity on T1- or T2-weighted images and contrast enhancement.

We think that balloon length could also be a factor for future investigation, but this was not assessed in our study. Although the balloons were all 2 cm in length, balloons of 7-mm diameter were used in four animals and balloons of 4-mm diameter were used in two animals.

After the 4-hour imaging time (including time before and during balloon inflation), all animals were immediately killed and autopsy was performed for removal of the spinal cord. All spinal cords were placed in formalin and submitted for pathologic examination. After formalin fixation, specimens were sectioned and processed to paraffin and slides were stained with hematoxylin and eosin and immunostained with an antibody for neuron beta amyloid precursor protein. Microscopic examination was subsequently performed by using the prepared slides.

Results

Six animals underwent successful balloon inflation. In one animal, a valve malfunction in the inflation device prevented measurement of pressure. Full inflation was achieved, however, based on MR imaging results. One animal underwent inflation at 6 atm, which we thought resulted in an incomplete inflation (animal 4). All other balloons were inflated to 10 atm. All six animals survived to complete the 4-hour imaging time. Because of the 4-hour limit of magnet availability, variations in post-deflation imaging times were caused by variations in the point in time during the 4 hours at which the balloon was inflated. No animals had spinal cord laceration or other evidence of injury below the level of balloon inflation that would suggest injury from catheterization.

T1- and T2-weighted images of the spinal cord were acquired of all six animals. MR imaging results and histopathologic findings of each animal are reported in Table 1. The total follow-up imaging time after deflation of the balloon ranged from 1.35 to 2 hours in five animals and was 1 hour 35 minutes in one animal (animal 3).

In two animals (animals 3 and 4) with 7-mm balloons, no signal intensity abnormality was noted on the MR images despite significant axonal and hemorrhagic injury revealed by histopathologic examination (Fig 2). For two animals with 7-mm balloons (animals 5 and 6), increased signal intensity was seen on the unenhanced T1-weighted images, suggesting hemorrhage; enhancement was observed on the T1-weighted images of two (animals 3 and 5). For one animal with a 4-mm balloon (animal 1), no abnormality was seen either histopathologically or by signal intensity on any sequence. For the final animal (ani-

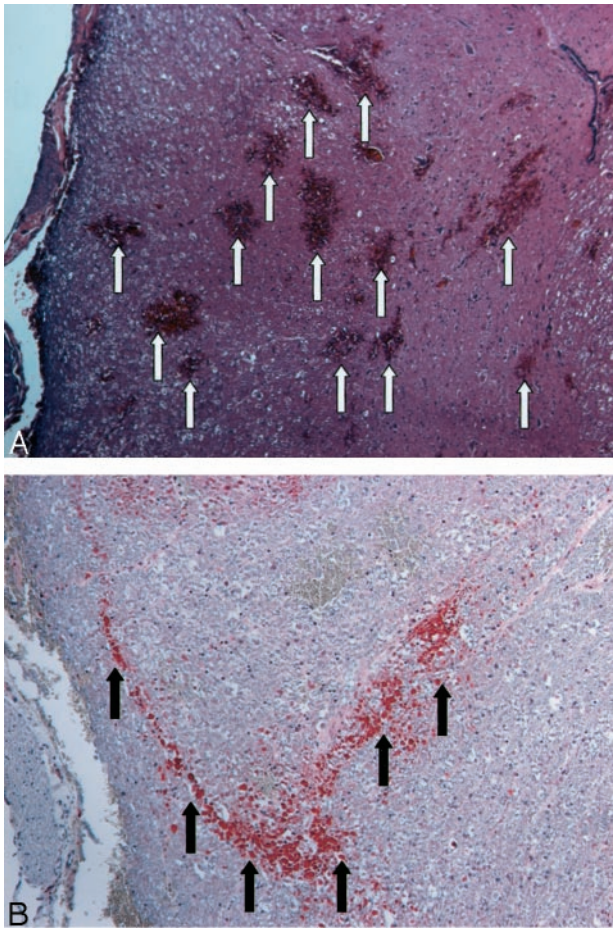

FIG 2. Images of animal 4.

A, Example of hematoxylin and eosin staining obtained at the level of the balloon. Multiple regions of petechial hemorrhage are indicated by *arrows*. Petechial hemorrhage is a characteristic of spinal cord contusion.

B, Beta amyloid precursor protein immunostaining of the region shown in *A*. Amyloid precursor protein is synthesized in neurons in the CNS and peripheral nervous system and is transported to the nerve endings from the cell body. Amyloid precursor protein accumulates when axoplasmic flow is disrupted; it is therefore a sensitive marker of axonal injury. Regions of stain accumulation (*arrows*) indicate posterior axonal injury.

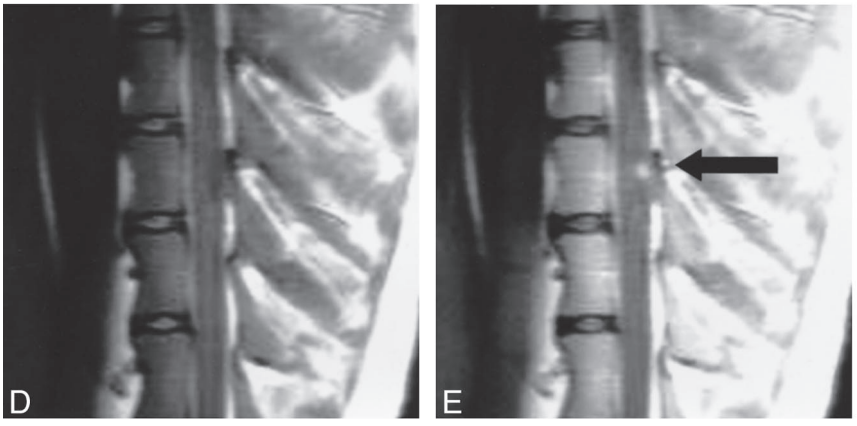

FIG 3. Images of animal 3.

A, Example of axial view T2-weighted MR image obtained at the level of balloon inflation after the balloon was deflated and removed. The cord displays homogenous signal intensity with no signal intensity change in the dorsal region that shows contrast enhancement in *C*.

B, Unenhanced T1-weighted MR image obtained in the axial plane at the level of balloon inflation. No abnormal signal intensity is seen in the spinal cord.

C, Contrast-enhanced T1-weighted MR image of the region shown in *B*. A large region of enhancement is located at the dorsal region of the spinal cord (*arrow*).

D, Unenhanced sagittal view T1-weighted MR image of the region shown in *B*. Note that no abnormal signal intensity is seen in the spinal cord.

E, Focal enhancement is observed after the injection of contrast material (*arrow*).

F, Hematoxylin and eosin staining of the spinal cord shows parenchymal hemorrhage in the peripheral white matter (*arrows*).

G, Beta amyloid precursor protein immunostaining of the region shown in *B* highlights well-developed axonal swellings (stain accumulation) in the cross section (*arrow*).

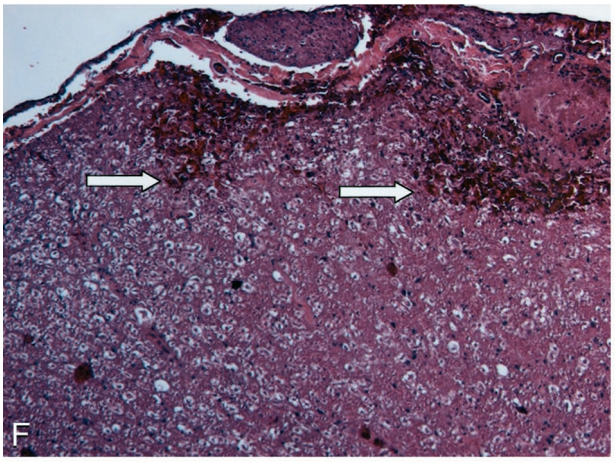

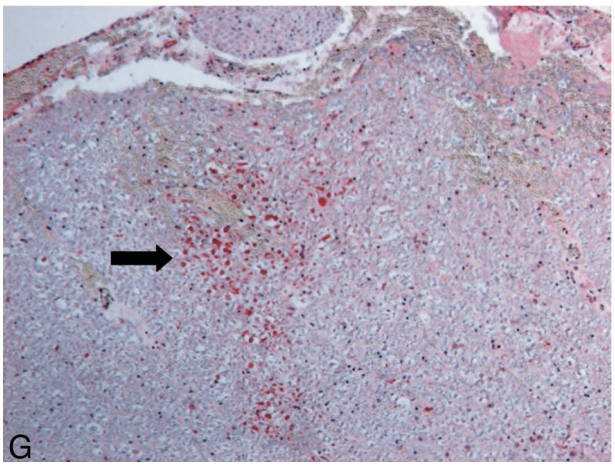

mal 2), T1 signal intensity and amyloid precursor protein staining were positive. In some cases, spinal cord expansion was questioned but no signal intensity changes were seen; those findings were therefore not considered reliably positive.

The spinal canal occlusion, MR imaging findings, contrast enhancement, and presence of hemorrhage and axonal injury revealed by histopathologic examination are summarized in Table 1. An example of contrast enhancement on the images of an animal with no injury revealed by T1- and T2-weighted imaging and the associated histopathologic findings are shown in Figure 3.

Discussion

The ideal model of a closed spinal cord injury with a shock component does not yet exist short of impact loading on the spinal column, and these studies are both difficult to perform and difficult to control from a research standpoint. Our model does not have a shock transmission feature, although there are strong histopathologic similarities between our spinal cord injury and the spontaneous injuries seen in humans with shock transmission injuries. A system with a water hammer type balloon may be possible but was not part of this investigation.

Although extensive literature on surgical weight-drop models is available, a relative paucity of literature on models that use balloons is available. Martin et al (19) described a model that uses rats with laminectomy and dural exposure for balloon introduction, but MR imaging was not performed in that study. Oro et al (20) described a balloon compression device in rats attached to spinous processes above and below an extensive laminectomy extending from C5 to T1, and, likewise, no MR imaging examination was performed. Sato et al (21) and Konno et al (22) studied compression in the dog cauda equina by using a midline insertion of a balloon in the lumbar canal via laminectomy of the L6 vertebra and the upper part of the sacrum, with the balloon inserted under the intact L7 lamina to produce the compression. Hence, that was another surgical model involving the cauda equina and not the spinal cord. Kuchner et al (23) drilled a small hole in the midline at T13 in a series of dogs and introduced an epidural balloon to achieve compression. This model probably most closely resembles that proposed herein; however, their model was an epidural compression model rather than a subarachnoid compression model and they did not pursue imaging studies. Their model requires entry at the site of the bony drilling, whereas our model permits navigation from a lumbar puncture to any site within the spinal column.

Our model offers several advantages over the surgical weight-drop models. First, with this percutaneous procedure, no bone is removed and there is theoretically a lower risk of infection in survival experiments. The method is easily performed under fluoroscopic monitoring. The injury has a high degree of control: balloons are readily available in a wide range of diameters and lengths, catheters are available in a wide range of styles, and the pressure and duration of inflation are easily modified and monitored. Although it is a pure model of extra-axial spinal cord compression, the technique offers the opportunity to obtain images before, during, and after injury by using conventional clinical devices at commercial field strengths with software that is directly applicable to the clinical setting.

Although the canine is the only animal in which this technique has been pursued, we know of no theoretical reason that other animal models could not be amenable. The use of the lateral foraminal approach for the puncture is a drawback insofar as there are spinal nerves and vessels that are not present in humans when a midline lumbar puncture is performed. However, in comparison to the drawbacks of the surgical laminectomy models enumerated above, the trade-off is minimal for the applications advocated herein.

One technical difference observed in dogs in comparison with human lumbar puncture is the tendency in dogs for the dura to pull away from the wall of the spinal canal during needle introduction. Verification of subarachnoid placement is critical, and we have seen extensive epidural passage of a wire before discovery of the error.

Survival studies should be at least as easy with this model as with others, because the models create spinal cord injury and the spinal cord care is similar regardless of how the injury was created. There is theoretical advantage to our model in that the risk of infection is minimal because of the percutaneous approach, but that remains to be shown.

Neurons in the CNS and peripheral nervous system synthesize amyloid precursor protein (24–29). Amyloid precursor protein is transported to nerve endings from the cell body by fast anterograde axonal transport (30, 31). It accumulates when axoplasmic flow is disrupted (32) and is therefore a sensitive marker of axonal injury (30, 33–37). Expression of amyloid precursor protein is shown to occur during the early stages of brain damage (24). In patients with head trauma who survived $\leq$3 hours, amyloid precursor protein was documented as a marker of axonal injury (35–37). Yam et al (30) studied focal ischemic lesions in rats and showed that the amount of amyloid precursor protein accumulation is determined by lesion size. Amyloid precursor protein immunoreactivity has been suggested to occur during the early stage of trauma and to decrease during the chronic stage.

The histopathologic examination of the spinal cords as the gold standard for documentation of injury was important in our study, both for purposes of showing similarity to clinically encountered injuries and for validation of imaging findings or indication of imaging shortcomings. Although the goal in this study was to document the validity of the model, the additional information provided by staining for axonal injury offered a powerful tool for understanding the cellular phenomena underlying the MR imaging findings. More studies, however, are needed. This study

did not assess, for instance, the relative sensitivities of MR imaging techniques to axonal injury versus edema versus hemorrhage versus the breakdown in the spinal cord of its equivalent to the blood-brain barrier, typically thought to be the cause of contrast enhancement in the brain. In the acute state, the sensitivity of MR imaging to axonal injury is at best speculative when using current techniques. Histopathologic examination was much more sensitive than MR imaging during the acute phase to show the different levels of injury between the two balloon sizes. Although the histopathologic techniques used in this study can also be applied in studies that use rodents or other small species, we think that the scattered patches of hemorrhage or amyloid precursor protein accumulation in variable regions of a cross section of the spinal cord in the hyperacute state are more readily documented with larger spinal cords on a volume basis alone. The canine spinal cord is, by its nature, more readily analogous to the human spinal cord both for histopathologic and imaging evaluation in terms of the range and variability of findings produced by a particular trauma. We acknowledge that considerable valuable work has been conducted using rodents, but the work described herein could not have been conducted in smaller species using instruments having direct translation into the human clinical setting. Although high field strength (eg, 4T and higher), small bore magnets offer value from a research standpoint, it is relevant to have experimental information regarding the histopathologic meaning of imaging findings from instruments used for patients (eg, meter bore, 0.5–3T). We think this study supports the use of larger species for collection of that information.

Previous MR imaging studies have evaluated the acute, subacute, and chronic phases of spinal cord injury. The timing of initial MR imaging changes due to edema or hemorrhage is reported to vary between 2 hours and 2 days (8, 12, 16, 17). MR imaging findings of spinal cord injury during the hyperacute phase recently have been reported. Bilgen et al (17) obtained MR images of the spinal cord as early as 9 minutes to 60 minutes after spinal cord trauma in rats. The earliest MR imaging finding of hemorrhage was detected 12 minutes after injury. In another study by Bilgen et al (16), contrast enhancement was observed during the hyperacute phase of spinal cord injury. A positive correlation between the volume of enhancement and the Tarlov score also was reported. These two studies (16, 17) showed the presence of MR imaging findings during the very early phase of spinal cord injury. However, these studies did not obtain images during the hyperacute phase (<2 hours). Abnormal MR imaging findings were present for every animal studied; nonetheless, these experiments investigated only severe spinal cord injury. To the best of our knowledge, no MR imaging studies have been conducted of spinal cord injury due to the graded degree of spinal cord compression ranging from minor to severe. Controlled studies of spinal cord injury with graded trauma will provide better understanding of the association between MR imaging changes and the degree of injurious insult.

Although we saw no evidence of injury remote from the area around the balloon inflation, injury from the catheterization process is a concern. Hamada et al (38) reported catheterization to the cisterna magna in humans without injury. Survival studies will be needed to fully address this concern.

This study raises many technical imaging questions. The disparity between the paucity of findings on the MR images in the absolute moments of injury compared with the substantial, grossly obvious hemorrhagic injury in the spinal cord tissue indicates a need for greater understanding of these events from MR physics and sequence selection standpoints. Also, separation of effects of physical compression of the spinal cord versus vascular effects from the time of compression versus reperfusion injury from balloon deflation requires further study. Ultra-short balloon inflations may avoid vascular effects, but the combined effects with longer inflations will be difficult to separate, as is also the case in the clinical situation. Furthermore, more studies with more delays in imaging need to be conducted, as do comparative evaluations at different field strengths. The model should be amenable to establishment of the degree of compression that is well tolerated and the gradation of injuries relative to time and degree of compression. We postulate that the model ultimately will allow for study of the "injury penumbra" of the spinal cord relative to those features and for the study of therapeutic interventions to alter that penumbra, in particular by using the techniques enabled by percutaneous intraspinal navigation.

We were surprised at several features during this study. First, navigation of the subarachnoid space with a guidewire once it was directed superiorly from the lateral puncture was relatively easy. Using fluoroscopic guidance, it was possible to direct either anterior or posterior to the spinal cord. Separation of the catheterization process from the balloon inflation process was difficult after the fact, but we saw no evidence of injury to the spinal cords remote from the region of balloon inflation on MR images and histopathologic examination revealed the injury to be limited to the area of balloon inflation despite the midthoracic placement of the balloons. Thus, in the lower areas of the spinal cord that were traversed with the catheter but not subjected to the balloon, the cords looked uninjured.

Second, there was a surprising paucity of immediate changes in the spinal cords on the MR imaging studies. Some cords exhibited changes during the observation period and ultimately showed hematoma or contrast enhancement, but the changes were much less marked than we thought they would be based on the degree of compression. Of the four animals for which histopathologic examination documented parenchymal hemorrhage, two showed evidence of hemorrhage and one cord appeared expanded but showed no signal intensity changes on MR images. In at least one animal (animal 3), no abnormality was seen on

MR images despite significant axonal injury and hemorrhage revealed by histopathologic examination. The acute MR imaging findings alone warrant further investigation with different balloon sizes and different inflation times during longer periods of observation.

The contrast enhancement seen in the spinal cord is of significant interest but is somewhat puzzling. The timing of the imaging (hyperacute) argues against breakdown of the blood-brain (spinal cord) barrier. Reactive hyperemia due to reperfusion of a cord that was ischemic during compression is another option. Further study is needed in more animals to confirm the reliability of the finding.

The balloons were easily localized by the signal intensity voids of the platinum markers on either end, even before inflation, and the catheter shafts were visible on axial view images. Also, the navigation need not have ended at the midthoracic level. On several occasions, the guidewire was advanced without difficulty as high as the cervical spine. We have also performed intraspinal navigation in human cadavers from a lumbar puncture into multiple locations in the subarachnoid space surrounding the brain and into the ventricular system. Thus, the study of injury at different levels of the spinal cord with different degrees of injury for different lengths of time is enabled by this technique, with each factor under operator control.

The discordance between histopathologic findings and MR imaging findings of hyperacute injury is also interesting. Further investigation is needed with longer observation times to better determine the temporal sensitivity of MR imaging for acute spinal cord injury. Differences between imaging during compression versus imaging after relief of compression warrant investigation. It is interesting that the only animal with a 7-mm balloon that had no injury revealed by MR imaging underwent inflation at 6 atm. Again, more data regarding the influence of inflation pressure is needed to understand that factor.

We agree that many cellular level studies could and should be performed in smaller species. However, unless we are to take treatments directly from mice or rats to humans, well-characterized intermediate models with understood histopathology and imaging appearances are needed. Further evaluation and characterization of this model is warranted.

Conclusion

We have shown the feasibility of a spinal cord injury model by using percutaneous intraspinal navigation that provides a graduated, controlled degree of spinal cord compression. Histopathologic examination of the spinal cord documented axonal injury or hemorrhage in all experiments that used 7-mm balloons and in one of two experiments that used 4-mm balloons. MR imaging documented spinal cord trauma findings of increased signal intensity on T1-weighted images in three of five animals with histopathologic injury. Enhancement was seen in two of five animals (one showed both T1 changes and enhancement). No abnormality was seen in one of five. T2 signal intensity increase was not observed for any animal. The potential of this model to investigate the sensitivity and specificity of different MR images in detecting varying degrees of acute spinal cord injury as documented with histopathologic examination merits further investigation.

Acknowledgments

We thank Leslie Mihal for assistance in the preparation of this manuscript and Virginia Barnett and Dorothy Smith for photographic assistance. We also thank Toshiba America Medical Systems (Tustin, CA) for research support in our angiography laboratory.

References

1. Allen AR. **Surgery of experimental lesion of spinal cord equivalent to crush injury of fracture dislocation of spinal column.** *JAMA* 1911;57:878–880
2. Alderman JL, Osterholm JL, D'Amore BR, Moberg RS, Irvin JD. **Influence of arterial blood pressure upon central hemorrhagic necrosis after severe spinal cord injury.** *Neurosurgery* 1979;4:53–55
3. Martinez LJ, Alderman JL, Kagan RS, Osterholm JL. **Spatial distribution of edema in the cat spinal cord after impact injury.** *Neurosurgery* 1981;8:450–453
4. Schouman-Claeys E, Frijas G, Cuenod CA, Begon D, Paraire F, Martin V. **MR imaging of acute spinal cord injury: results of an experimental study in dogs.** *AJNR Am J Neuroradiol* 1990;11:959–965
5. Falconer JC, Narayana PA, Bhattacharjee MB, Liu SJ. **Quantitative MRI of spinal cord injury in a rat model.** *Magn Reson Med* 1994;32:484–491
6. Hackney D, Ford JC, Markowitz RS, Hand CM, Joseph PM, Black P. **Experimental spinal cord injury: imaging the acute lesion.** *AJNR Am J Neuroradiol* 1994;15:960–961
7. Narayana PA, Kudrle WA, Liu SJ, Charnov JH, Butler BD, Harris JH Jr. **Magnetic resonance imaging of hyperbaric oxygen treated rats with spinal cord injury: preliminary studies.** *Magn Reson Imaging* 1991;9:423–428
8. Weirich SD, Cotler HB, Narayana PA, et al. **Histopathologic correlation of magnetic resonance imaging signal patterns in a spinal cord injury model.** *Spine* 1990;15:630–638
9. Ford JC, Hackney DB, Alsop DC, et al. **MRI characterization of diffusion coefficients in a rat spinal cord injury model.** *Magn Reson Med* 1994;31:488–494
10. Fukuoka M, Matsui N, Takanobu O, Murakami M, Seo Y. **Magnetic resonance imaging of experimental subacute spinal cord compression.** *Spine* 1998;23:1540–1549
11. Li GL, Farooque M, Holtz A, Olsson Y. **Apoptosis of oligodendrocytes occurs for long distances away from the primary injury after compression trauma to rat spinal cord.** *Acta Neuropathol (Berl)* 1999;98:473–480
12. Ohta K, Fujimura Y, Nakamura M, Watanabe M, Yato Y. **Experimental study on MRI evaluation of the course of cervical spinal cord injury.** *Spinal Cord* 1999;37:580–584
13. Perdiki M, Farooque M, Holtz A, Li GL, Olsson Y. **Expression of endothelial barrier antigen immunoreactivity in blood vessels following compression trauma to rat spinal cord.** *Acta Neuropathol (Berl)* 1998;96:8–12
14. Duncan EG, Lemaire C, Armstrong RL, Tator CH, Potts DG, Linden RD. **High-resolution magnetic resonance imaging of experimental spinal cord injury in the rat.** *Neurosurgery* 1992;31:510–519
15. Schwartz ED, Yezierski RP, Pattany PM, Quencer RM, Weaver RG. **Diffusion-weighted MR imaging in a rat model of syringomyelia after excitotoxic spinal cord injury.** *AJNR Am J Neuroradiol* 1999;20:1422–1428
16. Bilgen M, Abbe R, Narayana PA. **Dynamic contrast-enhanced MRI of experimental spinal cord injury: in vivo serial studies.** *Magn Reson Med* 2001;45:614–622
17. Bilgen M, Abbe R, Liu SJ, Narayana PA. **Spatial and temporal evolution of hemorrhage in the hyperacute phase of experimental spinal cord injury: in vivo magnetic resonance imaging.** *Magn Reson Med* 2000;43:594–600

18. Fujii H, Yone K, Sakou T. **Magnetic resonance imaging study of experimental acute spinal cord injury.** *Spine* 1993;18:2030–2034
19. Martin D, Schoenen J, Delree P, et al. **Experimental acute traumatic injury of the adult rat spinal cord by a subdural inflatable balloon: methodology, behavioral analysis and histopathology.** *J Neurosci Res* 1992;32:539–550
20. Oro JJ, Gibbs SR, Haghighi SS. **Balloon device for experimental graded spinal cord compression in the rat.** *J Spinal Disord* 1999; 12:257–261
21. Sato K, Konno S, Yabuki S, Mao GP, Olmarker K, Kikuchi S. **A model for acute, chronic, and delayed graded compression of the dog cauda equina: neurophysiologic and histologic changes induced by acute, graded compression.** *Spine* 1995;20:2386–2391
22. Konno S, Yabuki S, Sato K, Olmarker K, Kikuchi S. **A model for acute, chronic, and delayed graded compression of the dog cauda equina: presentation of the gross, microscopic, and vascular anatomy of the dog cauda equina and accuracy in pressure transmission of the compression model.** *Spine* 1995;20:2758–2764
23. Kuchner EF, Hansebout RR, Pappius HM. **Effects of dexamethasone and of local hypothermia on early and late tissue electrolyte changes in experimental spinal cord injury.** *J Spinal Disord* 2000; 13:391–398
24. Kawarabayashi T, Shoji M, Harigaya Y, Yamaguchi H, Hirai S. **Expression of APP in the early stage of brain damage.** *Brain Res* 1991;563:334–338
25. Bendotti C, Forloni GL, Morgan RA, et al. **Neuroanatomical localization and quantification of amyloid precursor protein mRNA by in situ hybridization in the brains of normal, aneuploid, and lesioned mice.** *Proc Natl Acad Sci U S A* 1988;85:3628–3632
26. Card JP, Meade RP, Davis LG. **Immunocytochemical localization of the precursor protein for β-amyloid in the rat central nervous system.** ***Neuron*** 1988;1:835–846
27. Kawarabayashi T, Shoji M, Harigaya Y, Yamaguchi H, Hirai S. **Amyloid β/A4 protein precursor is widely distributed in both the central and peripheral nervous systems of the mouse.** *Brain Res* 1991;552:1–7
28. Mita S, Schon EA, Herbert J. **Widespread expression of amyloid beta-protein precursor gene in rat brain.** *Am J Pathol* 1989;135: 1253–1261
29. Shivers BD, Hilbich C, Multhaup G, Salbaum M, Beyreuther K, Seeburg PH. **Alzheimer's disease amyloidogenic glycoprotein: expression pattern in rat brain suggests a role in cell contact.** *EMBO J* 1988;7:1365–1370
30. Yam PS, Takasago T, Dewar D, Graham DI, McCulloch J. **Amyloid precursor protein accumulates in white matter at the margin of a focal ischaemic lesion.** *Brain Res* 1997;760:150–157
31. Koo EH, Sisodia SS, Archer DR, et al. **Precursor of amyloid protein in Alzheimer disease undergoes fast anterograde axonal transport.** *Proc Natl Acad Sci U S A* 1990;87:1561–1565
32. Ichihara N, Wu J, Chui DH, Yamazaki K, Wakabayashi T, Kikuchi T. **Axonal degeneration promotes abnormal accumulation of amyloid β-protein in ascending gracile tract of gracile axonal dystrophy (GAD) mouse.** *Brain Res* 1995;695:173–178
33. Koizumi H, Povlishock JT. **Posttraumatic hypothermia in the treatment of axonal damage in an animal model of traumatic axonal injury.** *J Neurosurg* 1998;89:303–309
34. Blumbergs PC, Scott G, Manavis J, Wainwright H, Simpson DA, McLean AJ. **Staining of amyloid precursor protein to study axonal damage in mild head injury.** *Lancet* 1994;344:1055–1056
35. Gentleman SM, Roberts GW, Gennarelli TA, et al. **Axonal injury: a universal consequence of fatal closed head injury?** *Acta Neuropathol (Berl)* 1995;89:537–543
36. McKenzie KJ, McLellan DR, Gentleman SM, Maxwell WL, Gennarelli TA, Graham DI. **Is β-APP a marker of axonal damage in short-surviving head injury?** *Acta Neuropathol (Berl)* 1996;92: 608–613
37. Sherriff FE, Bridges LR, Gentleman SM, Sivaloganathan S, Wilson S. **Markers of axonal injury in post mortem human brain.** *Acta Neuropathol (Berl)* 1994;88:433–439
38. Hamada J, Mizuno T, Kai Y, Morioka M, Ushio Y. **Microcatheter intrathecal urokinase infusion into cisterna magna for prevention of cerebral vasospasm: preliminary report.** *Stroke* 2000;31:2141–2148